Supporting Information for

CHANS-SD-YRB V1.0: A System Dynamics model of the coupled human-natural systems for the Yellow River Basin

Shan Sang[1,2], Yan Li[1,2*], Shuang Zong[1,2], Lu Yu[1,2], Shuai Wang[1,2], Yanxu Liu[1,2], Xutong Wu[1,2], Shuang Song[1,2], Wenwu Zhao[1,2], Xuhui Wang[3], Bojie Fu[4]

[1]State Key Laboratory of Earth Surface Processes and Hazards Risk Governance (ESPHR), Beijing Normal University, Beijing, China

[2]Institute of Land Surface System and Sustainable Development, Faculty of Geographical Science, Beijing Normal University, Beijing, China

[3]Institute of Carbon Neutrality, Laboratory for Earth Surface Processes, College of Urban and Environmental Sciences, Peking University, Beijing 100871, China

[4]State Key Laboratory of Regional and Urban Ecology, Research Center for Eco-Environmental Sciences, Chinese Academy of Sciences, Beijing 100085, China

Corresponding Author:

Yan Li, Ph.D.

Institute of Land Surface System and Sustainable Development, Faculty of Geographical Science, Beijing Normal University, Beijing, 100875, China

Email: yanli.geo@gmail.com

Contents

S1. User guide for the CHANS-SD-YRB model

The CHANS-SD-YRB model version V1.0 was developed based on the VENSIM DSS 9.3 (Ventana Systems, 2023) software platform. The released model version V1.0 package includes model files for execution, simulation results files, and data files for validation (available at https://doi.org/10.5281/zenodo.17568963), as listed in Table S1.

Table S1 File description of the CHANS-SD-YRB V1.0 model

File name	Content	Note
CHANS_SD_YRB_V1.mdl	The model source file	Required for model execution
TENmodule_couple_his.vdfx	Simulation results for the historical period	
TENmodule_future_Baseline.vdfx	Simulation results for baseline scenario	
ture data.vdfx	Validation file for the historical period	
YRBdata_true2020.xls	Validation data for the historical period	
data_input_vensim.xls	Exogenous input data required for simulation	Required for model execution
parameters_in_model.xls	Summary of parameters in the model	

Ensure that all required files for model execution are in the same folder. Then, open **CHANS_SD_YRB_V1.mdl** using **Vensim DSS** software, click the **Run** button, and the model will execute. Note that the Vensim PLE allows users to view the model but does not support model execution.

S2. Full description of each sector

S2.1. Population

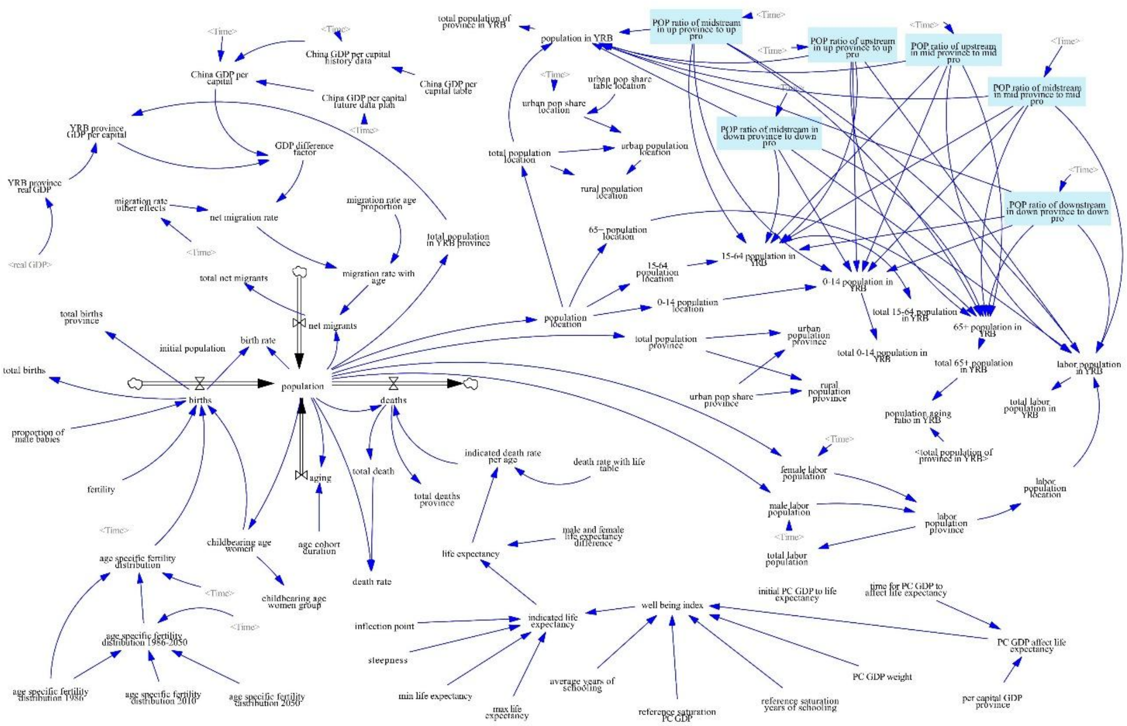

Figure S1 Model interface of the *Economy* sector

The total population (Equation S1) is categorized by individuals in one-year age groups and gender,

$$Pop_{g,a} = IniPop_{g,a} + \begin{cases} \int \left(B_{g,a} + NM_{g,a} - D_{g,a}\right)dt, & a = 0 \\ \int \left(Pop_{g,a} + NM_{g,a} - D_{g,a}\right)dt, & 1 \le a \le 99, a = 100\ and\ over \end{cases} \tag{S1}$$

where *Pop* is population, subscript g and a are gender (g = M is male, g = F is female) and age (a = 0-100 and over); $IniPop_{g,a}$ is the population in the initial year, $B_{g,a}$ is the births (a = 0), $D_{g,a}$ is the deaths, $NM_{g,a}$ is the net migrants (i.e., immigrants – emigrations).

Births (Equation S2) is driven by exogenous variables,

$$B_{g,a} = TFR \times \sum_{a=15}^{49}(Pop_{F,a} \times FD_a) \tag{S2}$$

where $Pop_{F,a}$ is the female at age a, with age between 15 and 49 considered as the female with fertility; *TFR* is total fertility rate, FD_a is the fertility probability of female at age a, from census yearbooks (NBSC, 2020b).

Deaths (Equation S3) is calculated by the West Life Table and life expectancy:

$$D_{g,a} = LT_a(LE_g) \tag{S3}$$

$$LE_g = \begin{cases} LE_I - 1.5, & g = male \\ LE_I + 1.5, & g = female \end{cases} \tag{S4}$$

where LT_a is the life table with death rate of age a, LE_g is the life expectancy of gender, the difference of the life expectancy for male and female is 3, according to T21-China model (Qu et al., 2020).

Life expectancy (Equation S5) is calculated by a function of human well-being

$$LE_I = LE_{min} + (LE_{max} - LE_{min}) \times \left(\frac{1}{e^{-step \times WBI} \times e^{inflection \times step} + 1} - \frac{e^{-step \times WBI}}{e^{inflection \times step} + 1}\right) \tag{S5}$$

where LE_I is the indicated life expectancy, LE_{min}, LE_{max}, step and *inflection* are the fitted minimum, maximum, curve steepness and inflection point, from historical data.

Human well-being (Equation S6) is calculated by economic and education level,

$$WBI = \left(\frac{PC_{GDP}}{Ref_{Income}}\right) \times w + \left(\frac{AYS}{SYS}\right) \times (1 - w) \tag{S6}$$

where *WBI* is the well-being index, the first half is income indicators, and the second half is educational indicators. PC_{GDP} is per capita GDP from the *Economy* sector; *AYS* is average years of schooling, from census yearbooks (NBSC, 2020b); Ref_{Income} is reference saturation income, *SYS* is saturation years of schooling, *w* is the weight of the income indicator, from T21-China model (Qu et al., 2020).

Migration (Equation S7) is influenced by regional economic development differences between inside and outside of the YRB,

$$NM_{g,a} = Pop_{g,a} \times MRP_{g,a} \times NMR \tag{S7}$$

$$NMR = \left(\frac{GDP_{PC_{YRB}} - GDP_{PC_{China}}}{GDP_{PC_{YRB}}}\right) \times OthEff \tag{S8}$$

where $MRP_{g,a}$ is the migration rate of each age group from census yearbooks (NBSC, 2020b); *NMR* is the net migration probability; $GDP_{PCChina}$ and GDP_{PCYRB} are the per capita GDP of China and the Yellow River Basin from the *Economy* sector; *OthEff* is the other influencing coefficient of mobility, calibrated from historical data.

S2.2. Economy

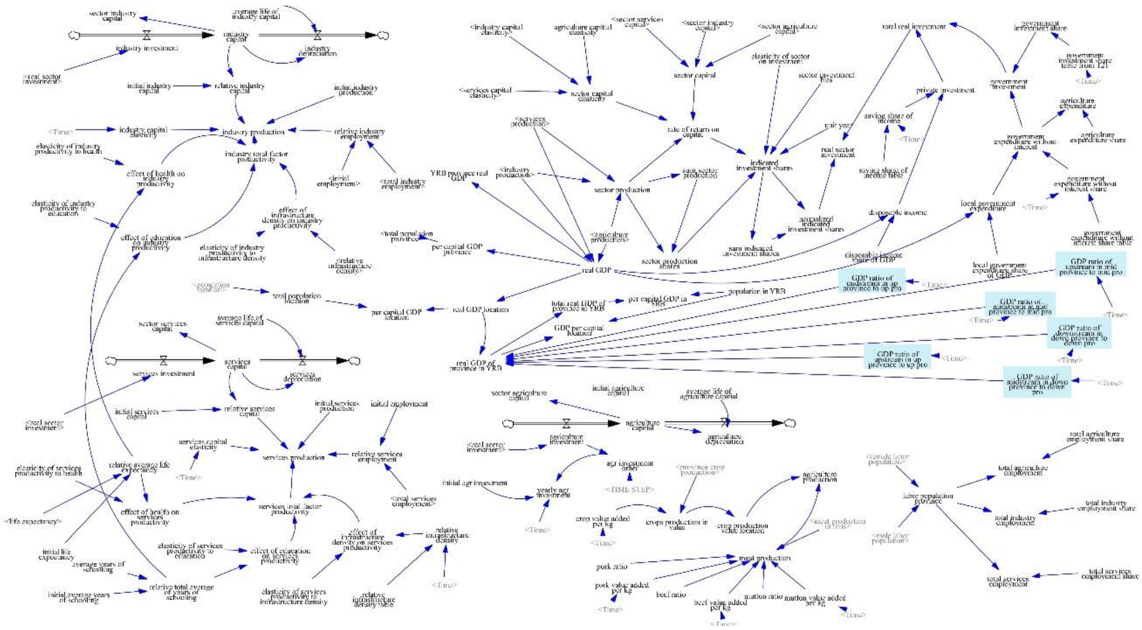

Figure S2 Model interface of the *Economy* sector

Gross product of industry and services (Equation S9) is calculated by Cobb-Douglas production function (Cobb and Douglas, 1928),

$$GDP_s = IniGDP_s \times TFP_s \times \left(\frac{L_s}{IniL_s}\right)^{1-\alpha_s} \times \left(\frac{K_s}{IniK_s}\right)^{\alpha_s} \tag{S9}$$

where *s* represents three industry sectors, agriculture, industry, and service; GDP_s is the gross domestic product in sector s, $IniGDP_s$ is the gross domestic product in the initial year; TFP_s is the total factor productivity; L_s is the labor force, $IniL_s$ is the labor force in initial year, from *Population* sector; α_s is capital elasticity, reflecting the elasticities of capital to production, $1\text{-}\alpha_s$ is labor elasticity, reflecting the elasticities of labor to production; K_s refers to the capital level, $IniK_s$ is the capital level in the initial year;

The total factor productivity (Equation S10) is calculated from exogenous (infrastructure, education, and elasticity), and endogenous variables (health and labor force),

$$TFP = Edu_{eff} \times Hea_{eff} \times Inf_{eff} \tag{S10}$$

$$Edu_{eff} = \left(\frac{AYS}{IniAYS}\right)^{\epsilon_1} \tag{S11}$$

$$Hea_{eff} = \left(\frac{ALE}{IniALE}\right)^{\epsilon_2} \tag{S12}$$

where Edu_{eff} represents the effect of education on total factor productivity, *IniAYS* is average years of schooling in the initial year, obtained from census yearbooks (NBSC, 2020b); Hea_{eff} represents the effect of health on total factor productivity, *ALE* is average life expectancy, *IniALE* is average life expectancy in the initial year from the *Population* sector; Inf_{eff} represents the effect of infrastructure on total factor productivity, ϵ_1 and ϵ_2 are the elasticities of total factor productivity to education and health, from T21-China model (Qu et al., 2020).

Capital level (Equation S13) is calculated by investment and capital depreciation,

$$K_S = IniGDP_S + \int (Invest_S - Depreciate_S)dt \tag{S13}$$

where $Invest_S$ is the investment (Equation S14), and $Depreciate_S$ is capital depreciation (Equation S16).

$$Invest_s = \sum_{S=1}^{3} GDP_s \times InvestR \times InvestShare_s \tag{S14}$$

$$InvestShare_s = \frac{GDP_S}{\sum_{S=1}^{3} GDP_S} \times (ROC_s)^{ElaRI_s} \tag{S15}$$

$$ROC_s = \frac{GDP_S \times \alpha_S}{K_S} \tag{S16}$$

$$Depreciate_S = \frac{K_S}{KAveLife} \tag{S17}$$

where *InvestR* is the ratio of investment to GDP, from the China Statistical Yearbook (NBSC, 2020c); $InvestShare_s$ is the investment share of each industry type; ROC_s is the rate of return on capital; $ElaRI_s$ is the elasticity of rate of return to investment; *KAveLife* is the average life of productive capital.

Gross agricultural production includes both crop and livestock production, determined by their respective prices,

$$GDP_{crop} = Crop_{pro} \times Price_C \tag{S18}$$

$$GDP_{livestock} = Livestock_{pro} \times Price_L \tag{S19}$$

where $Crop_{pro}$ is the crop production, and $Livestock_{pro}$ is the livestock production from the *Food* sector; $Price_C$ and $Price_L$ are the prices of crop and meat, from the China Statistical Yearbook (NBSC, 2020c).

S2.3. Energy

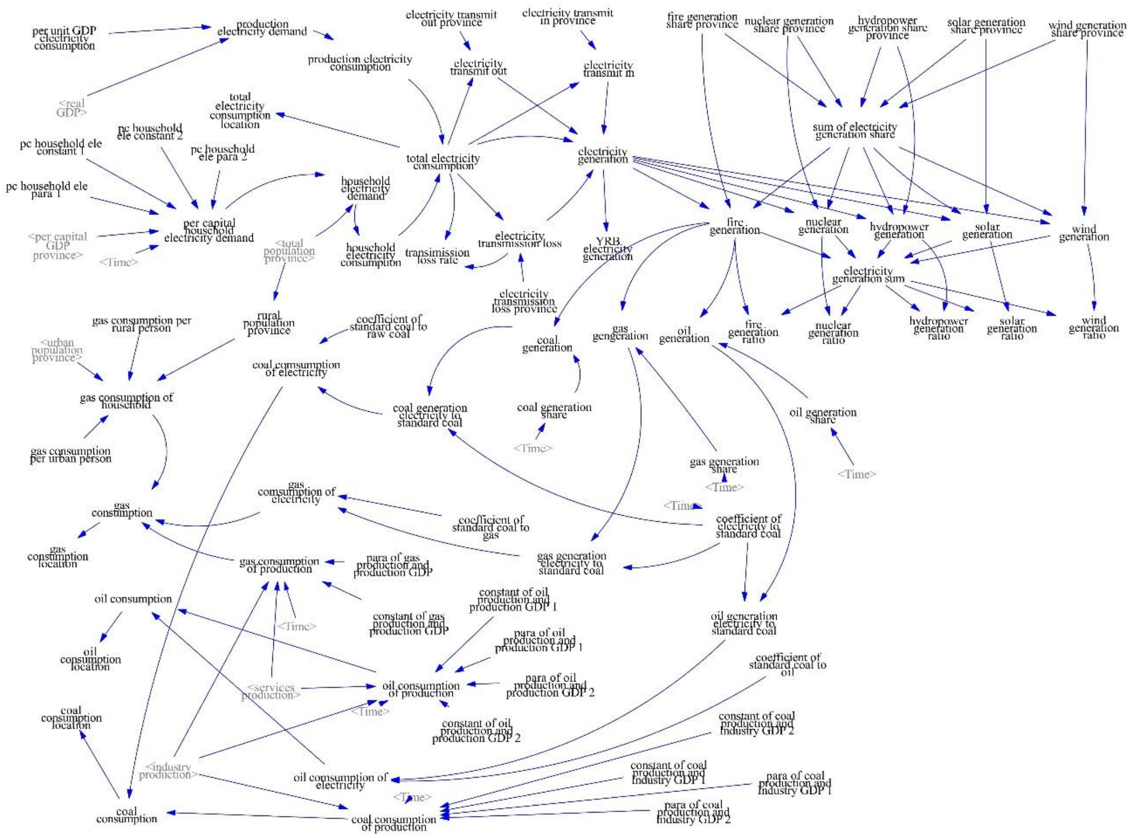

Figure S3 Model interface of *Energy* sector

Electricity generation includes residential and industrial production uses (Equations S20-S21), as well as cross-provincial electricity transmission from Energy Statistical Yearbook (NBSC, 2020a). The proportions of electricity derived from thermal, hydro, wind, solar, and nuclear sources are determined by specified ratios from the same yearbook:

$$Ele_{res} = Pop \times (Para_{RE} \times PC_{GDP} + Const_{RE}) \quad \text{(S20)}$$

$$Ele_{pro} = GDP \times EI \quad \text{(S21)}$$

where Ele_{res} is residential electricity consumption, *Pop* is from *Population* sector, PC_{GDP} and *GDP* are from *Economy* sector, $Para_{RE}$ and $Const_{RE}$ come from the slope and constant term of the linear fit between historical per capita GDP and per capita household electricity consumption. Ele_{pro} is production electricity consumption, and *EI* is the electricity intensity, indicating electricity consumption per unit of GDP, from the China Energy Statistical Yearbook (NBSC, 2020a).

Coal (Equation S22), oil (Equation S23) and gas (Equation S24) consumption are obtained from the linear fit of historical sector GDP and related consumption,

$$Coal_{con} = TP \times Share_{coal} \times Coef_{ESC} \times Coef_{SCC} + Para_{IC} \times GDP_{ind} + Const_{IC} \quad \text{(S22)}$$

$$Oil_{con} = TP \times Share_{oil} \times Coef_{ESC} \times Coef_{SCO} + Para_{ISO} \times (GDP_{ind} + GDP_{ser}) + Const_{ISO} \quad \text{(S23)}$$

$$Gas_{con} = TP \times Share_{gas} \times Coef_{ESC} \times Coef_{SCG} + Para_{ISG} \times (GDP_{ind} + GDP_{ser}) + Const_{ISG} + Pop_{rural} \times PCG_{rural} + Pop_{urban} \times PCG_{urban} \quad \text{(S24)}$$

where TP is the thermal power generation; $Share_{coal}$, $Share_{oil}$ and $Share_{gas}$ are the proportion of coal, oil and gas in thermal power generation; $Coef_{ESC}$ is the standard coal conversion coefficient of electricity, $Coef_{SCC}$, $Coef_{SCO}$ and $Coef_{SCG}$ are the conversion coefficients of standard coal, coal, oil and gas, which are derived from General Principles for the Calculation of Comprehensive Energy Consumption (GB/T 2589-2008, GB/T 2589-2020); $Para_{IC}$ and $Const_{IC}$ come from the slope and constant term from the linear fit of historical industrial GDP and coal industry consumption; $Para_{ISO}$ and $Const_{ISO}$ are similar parameters for oil industry consumption, and $Para_{ISG}$ and $Const_{ISG}$ for gas industry consumption; Pop_{rural} and Pop_{urban} are rural and urban population, from *Population* sector, PCG_{rural} and PCG_{urban} are the per capita natural gas consumption in rural and urban areas from the China Energy Statistical Yearbook (NBSC, 2020a).

S2.4. Food

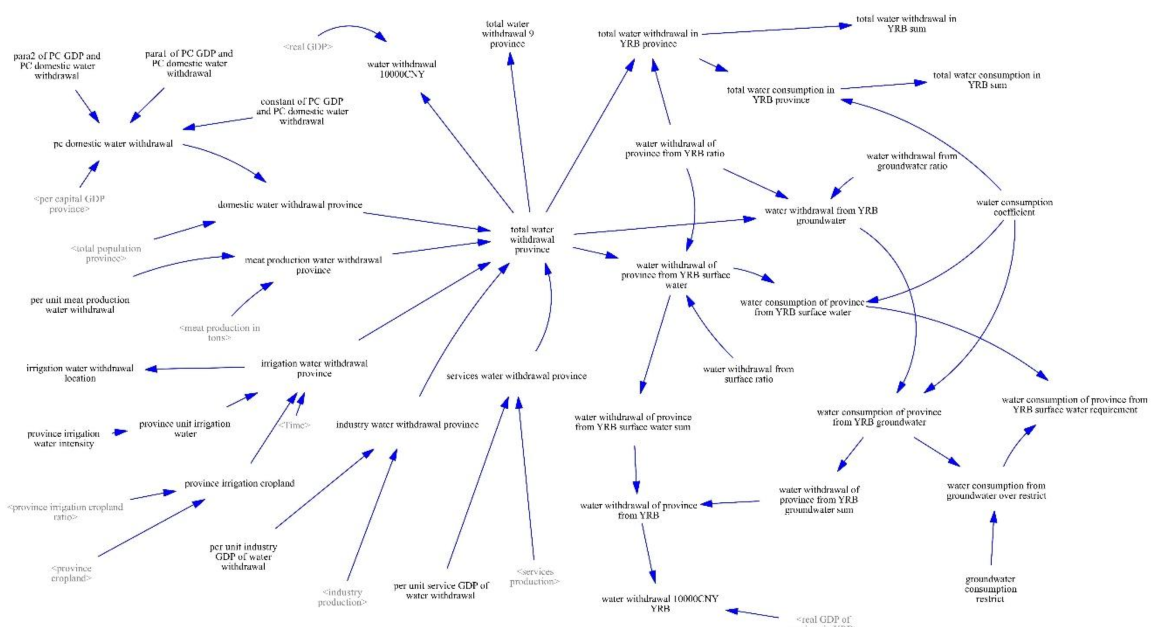

Figure S4 Model interface of *Food* sector

The *Food* sector simulates livestock and crop production ($Livestock_{pro}$ and $Crop_{pro}$), as well as food demand. Livestock production is calculated as a function of economic development and population growth (Equation S25),

$$Livestock_{pro} = Pop \times \left(Para_{GL1} + (Para_{GL2} - Para_{GL1}) \times \frac{PC_{GDP}}{PC_{GDP}+Const_{GL}}\right) \quad \text{(S25)}$$

where *Pop* is from *Population* sector, PC_{GDP} are from *Economy* sector; $Para_{GL1}$、$Para_{GL2}$ and $Const_{GL}$ are parameters obtained by fitting the historical per capita meat production and per capita GDP data.

Crop production (Equation S26) is determined by the crop yield ($Yield_c$) and harvested area (PA_c),

$$Crop_{pro} = \sum_{c=1}^{7} Yield_c \times PA_c \quad \text{(S26)}$$

$$PA_c = Area_{Cropland} \times CRI \times PR_c \quad \text{(S27)}$$

where *c* represents the crop type, including rice, wheat, maize, beans, cotton, potato and oil plants. PA_c is the harvest area of each crop, and $Area_{Cropland}$ is the cropland area from the *Land* sector; *CRI* is the multiple cropping index, and PR_c is the harvest ratio of each crop from the China Agricultural Yearbook (MAARA, 2020).

Crop yield is composed of a trend ($Yield_{ctrend}$) and an anomaly ($Yield_{canomaly}$) term,

$$Yield_c = Yield_{c_{trend}} + Yield_{c_{anomaly}} \quad \text{(S28)}$$

where $Yield_c$ is the yield of crop type *c*, the trend ($Yield_{ctrend}$) and anomaly ($Yield_{canomaly}$) of crop yield are fitted using historical data. Because the factors influencing long-term yield trends differ from those driving short-term fluctuations, they are modeled separately. The yield trend is determined by fertility use (Equation S29), which is also influenced by agricultural investment (Equation S30);

$$Yield_{c_{trend}} = Para_{c_{fer}} \times Fer_{unit} + Const_{c_{YT}} \quad \text{(S29)}$$

$$Fer_{unit} = Para_{IF} \times ln\left(\frac{Invest_{agr}}{CA}\right) + Const_{IF} \quad \text{(S30)}$$

where Fer_{unit} is fertilizer use intensity, $Para_{cfer}$ and $Const_{cYT}$ are parameters obtained by linear fitting of historical yield trend values with fertilizer use data. $Invest_{agr}$ is the agricultural investment, $Para_{IF}$ and $Const_{IF}$ are parameters obtained by fitting the historical fertilizer use intensity and investment data.

The crop yield anomaly is influenced by temperature and precipitation (Equation S31),

$$Yield_{c_{anomaly}} = Para_{c_{Tem}} \times Tem_P + Para_{c_{Pre}} \times Pre_P + Const_{c_{YA}} \quad \text{(S31)}$$

where Tem_P and Pre_P are the annual mean temperature and precipitation of each province, from *Climate* sector; $Para_{cTem}$, $Para_{cPre}$ and $Const_{cYA}$ are parameters obtained by linearly fitting historical yield anomaly values with temperature and precipitation data.

Food demand ($Crop_{dem}$) encompasses both staple and feed grain demand, which are determined by population size and dietary patterns,

$$Crop_{dem} = Crop_{human} + Crop_{livestock} \quad \text{(S32)}$$

where $Crop_{dem}$ is the total crop demand, $Crop_{human}$ is the human staple grain demand, $Crop_{livestock}$ is the feed grain demand.

Human staple grain demand includes three crops:

$$Crop_{human} = \sum_{d=1}^{3} Crop_{HD_d} \quad \text{(S33)}$$

$$Crop_{HD_d} = \frac{1}{CECF_d} \times \left(Daliy_{urban} \times Pop_{urban} \times 365 \times CDR_{f_{urban}} + Daliy_{rural} \times Pop_{rural} \times 365 \times CDR_{f_{rural}}\right) \times Coef_{FR_d} \quad \text{(S34)}$$

where d represents the staple grain type, cereals, beans, and potatoes; $Crop_{HDd}$ is human requirements for each staple grain; $CECF_d$ is the energy conversion coefficient for each staple grain, from the literature (Zhang et al., 2012); $Daily_{urban}$ is the daily calorie requirement per standard person in urban regions, CDR_{furban} is the proportion of staple grain in dietary of urban regions, $Daily_{rural}$ is the daily calorie requirement per standard person in rural regions, CDR_{frural} is the proportion of staple grain in dietary of rural regions, from the literature (Ju et al., 2018); $Coef_{FRd}$ is the conversion coefficient of each staple grain type from final grain to raw grain, from the literature (Zhang et al., 2012); Pop_{urban} and Pop_{rural} are population in urban and rural regions, from *Population* sector.

Feed grain demand considers three livestock:

$$Crop_{livestock} = \sum_{m=1}^{3} Crop_{LD_m} \quad \text{(S35)}$$

$$Crop_{LD_m} = \frac{1}{MECF} \times \left(Daliy_{urban} \times Pop_{urban} \times 365 \times MDR_{m_{urban}} + Daily_{rural} \times Pop_{rural} \times 365 \times MDR_{m_{rural}}\right) \times MR_m \times Coef_{FC_m} \quad \text{(S36)}$$

where m represents the livestock meat type, pork, beef, and mutton, $Crop_{LDm}$ is the feed grain requirement for each livestock; $MECF$ is energy conversion factors of animal-based foods, $Daily_{urban}$ is the daily calorie requirement per standard person of the staple grain in urban regions, MDR_{murban} is the proportion of animal-based food in dietary of urban regions, $Daily_{rural}$ is the daily calorie requirement per standard person of the staple grain in rural regions, MDR_{mrural} is the proportion of animal-based food in dietary of rural regions from the literature (Ju et al., 2018); MR_m is share of demand by livestock meat type, from the China Statistical Yearbook (NBSC, 2020c), $Coef_{FCm}$ is grain consumption coefficients of different livestock, from the literature (Zeng et al., 2021), Pop_{urban} and Pop_{rural} are population in urban and rural regions, from *Population* sector.

S2.5. Water Demand

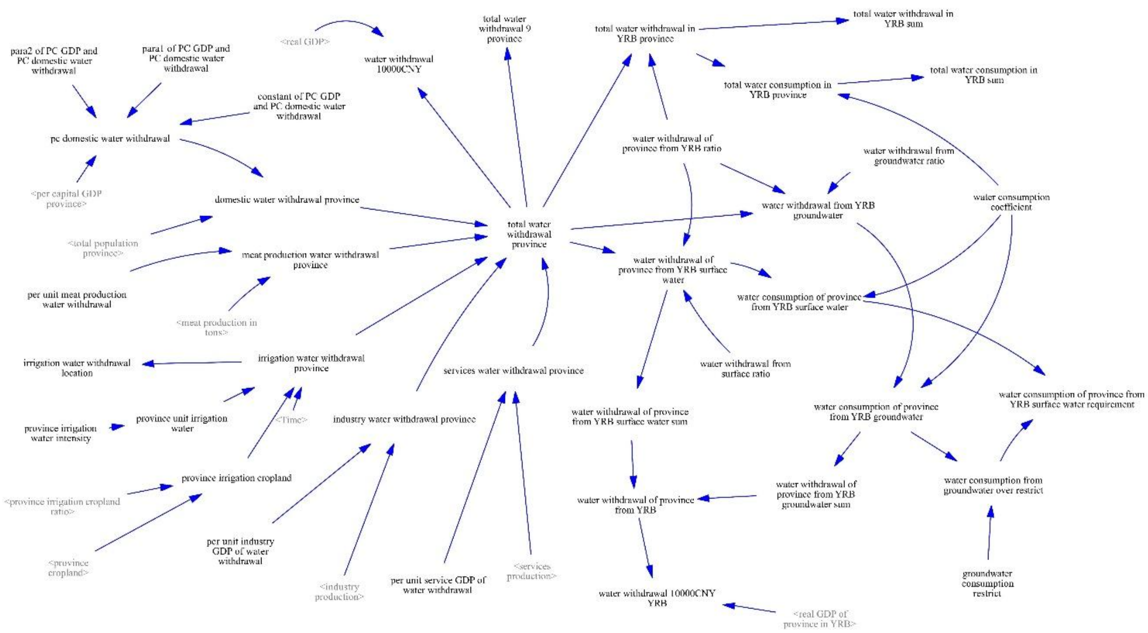

Figure S5 Model interface of *Water Demand* sector

The *Water Demand* sector simulates water withdrawal (*WW*) and consumption (*WC*) across multiple uses—agriculture (WW_{agr}), industry (WW_{ind}), services (WW_{ser}), and residential (WW_{res});

$$WC = WW \times WE \quad \text{(S37)}$$

$$WW = WW_{agr} + WW_{ind} + WW_{ser} + WW_{res} \quad \text{(S38)}$$

where *WC* is total water consumption, *WE* is water efficiency, from water resources bulletin (YRCCMWR, 2020).

Agricultural water withdrawal includes water for irrigation (WW_{irr}) and livestock (WW_{liv}),

$$WW_{agr} = WW_{irr} + WW_{liv} \quad \text{(S39)}$$

$$WW_{irr} = Irr_{unit} \times Area_{Cropland} \times IR \tag{S40}$$

$$WW_{liv} = LWW_{unit} \times Livestock_{pro} \tag{S41}$$

where irr_{unit} is irrigation water use intensity, $Area_{Cropland}$ is cropland area from *Land* sector, *IR* is irrigation cropland ratio, from the China Agricultural Yearbook (MAARA, 2020); LWW_{unit} is water use per unit of meat production, from the China Statistical Yearbook; $Livestock_{pro}$ is livestock production, from *Food* sector.

Industry, service, and residential water withdrawal are closely associated with economic development,

$$WW_{ind} = WWI_{ind} \times GDP_{ind} \tag{S42}$$

$$WW_{ser} = WWI_{ser} \times GDP_{ser} \tag{S43}$$

$$WW_{res} = Pop \times \left(Para_{GD1} + (Para_{GD2} - Para_{GD1}) \times \frac{PC_{GDP}}{PC_{GDP} + Const_{GD}}\right) \tag{S44}$$

where WWI_{ind} and WWI_{ser} are the water intensity of industry and service, from the China Statistical Yearbook (NBSC, 2020c), gross product of industry (GDP_{ind}) and service (GDP_{ser}) are from *Economy* sector; *Pop* comes from *Population* sector, PC_{GDP} comes from *Economy* sector; $Para_{GD1}$, $Para_{GD2}$ and $Const_{GD}$ are parameters obtained by fitting the historical per capita domestic water use with per capita GDP.

S2.6. Water Supply

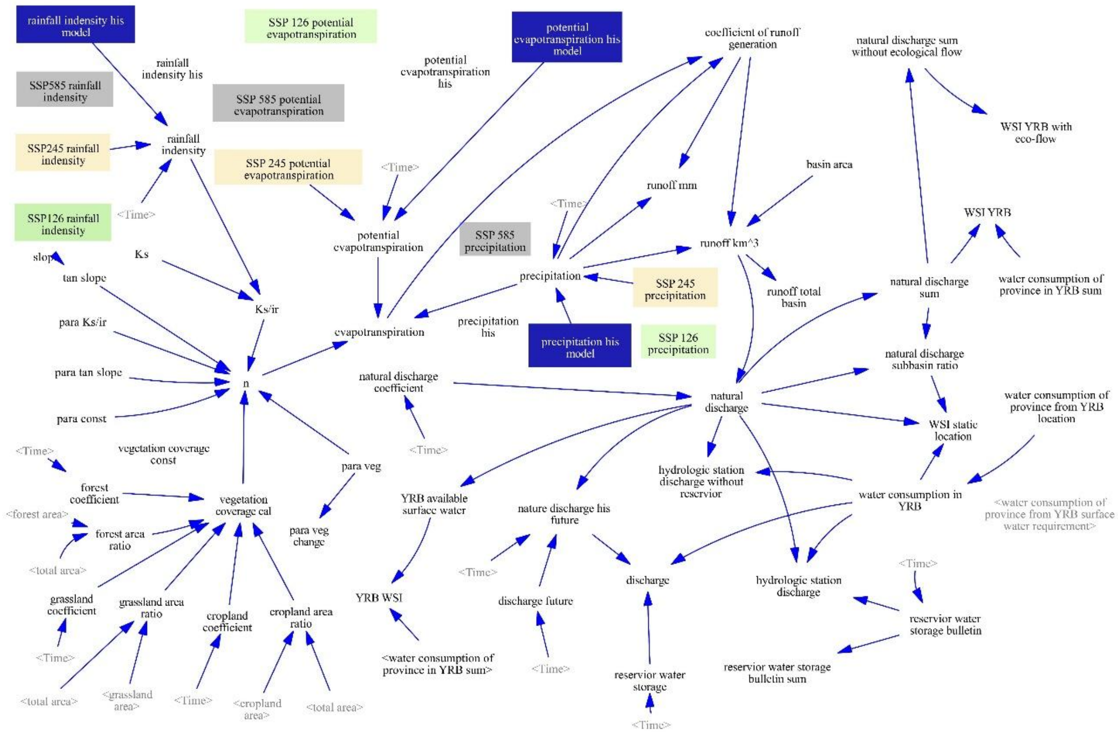

Figure S6 Model interface of *Water Supply* sector

The *Water Supply* sector simulates runoff, discharge, and their changes in each subbasin. Runoff (*R*) is determined by precipitation and evapotranspiration (*ET*) based on the water balance principle derived from the Budyko equation (Yang et al., 2009),

$$R = Pre - ET \tag{S45}$$

$$ET = \frac{EP \times Pre}{(PreS^{n} + PET^{n})^{\frac{1}{n}}} \tag{S46}$$

where *ET* is the evapotranspiration; *Pre* is the precipitation at sub-basin level, *PET* is potential evapotranspiration at sub-basin, both from *Climate* sector; *n* is a parameter reflecting the basin landscape characteristics.

The parameter *n* is related to saturated hydraulic conductivity (*Ks*), precipitation intensity (*PI*), average slope (*β*) and fraction of vegetation coverage (*FVC*),

$$n = Para_{E1} \times \left(\frac{Ks}{PI}\right)^{Para_{E2}} \times FVC^{Para_{E3}} \times e^{Para_{E4} tan\beta} \tag{S47}$$

$$FVC = Para_{Cropland} \times Area_{Cropland} + Para_{Forest} \times Area_{Forest} + Para_{Grassland} \times Area_{Grassland} \tag{S48}$$

where *ParaE1*, *ParaE2*, *ParaE3* and *ParaE4* are parameters fitted from historical data; *FVC* is calculated by area of cropland, forest and grassland, from *Land* sector, $Para_{Cropland}$,

$Para_{Forest}$ and $Para_{Grassland}$ are parameters calibrated based on historical remote sensing monitoring dataset (Jia et al., 2015, 2019; Xu et al., 2018).

Runoff and the loss coefficient ($Coef_{loss}$) (defined by the ratio of natural streamflow to runoff) determine the natural streamflow (*NS*) due to the water loss during the confluence process (Equation S49),

$$NS = R \times (1 - Coef_{loss}) \tag{S49}$$

where $Coef_{loss}$ is calculated using the China Natural Runoff Dataset (Gou et al., 2021) and Gauge-based Natural Streamflow Dataset (Miao et al., 2022).

Actual streamflow (*AS*) is the streamflow after considering the influence of human activities, i.e., human water consumption (*WC*) from the *Water Demand* sector, and it is then transferred through hydrological connectivity from upstream, to midstream, to downstream, and finally into the sea (Equation S50-S52),

$$AS_{up} = NS_{up} - WC_{up} \tag{S50}$$

$$AS_{mid} = NS_{mid} + AS_{up} - WC_{mid} \tag{S51}$$

$$AS_{down} = NS_{down} + AS_{mid} - WC_{down} \tag{S52}$$

where the actual streamflow in the upstream (AS_{up}) flows into the midstream, similarly, the actual streamflow in the midstream (AS_{mid}) flows into the downstream, the actual streamflow in the downstream (AS_{down}) is the streamflow into the sea.

S2.7. Sediment

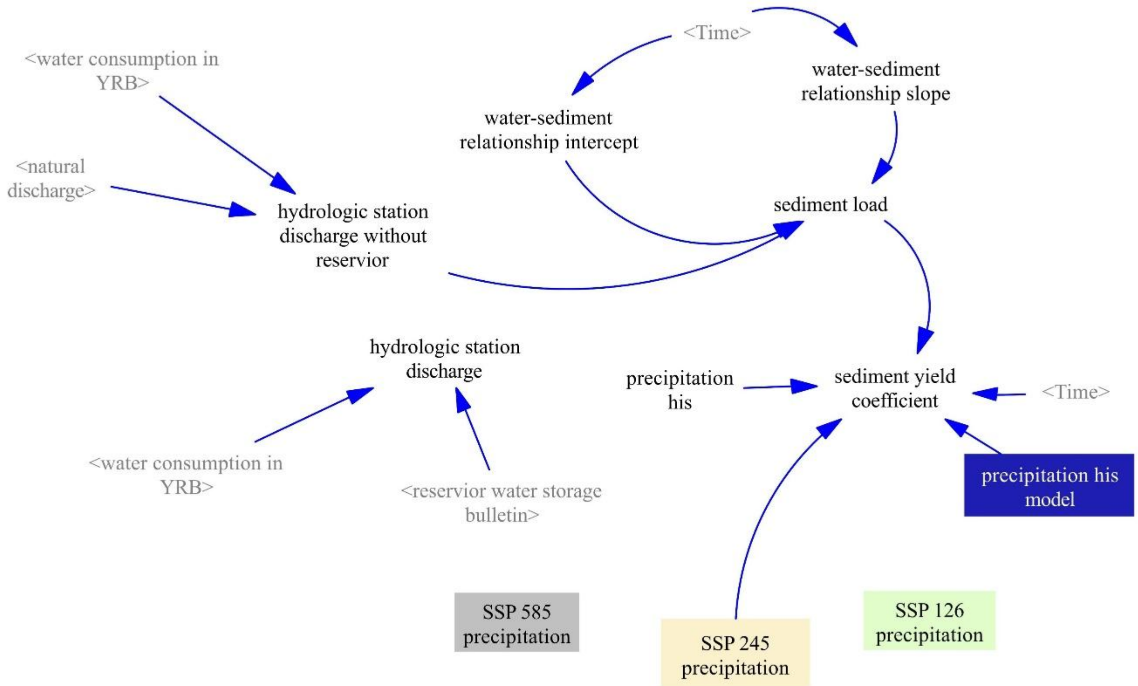

Figure S7 Model interface of *Sediment* sector

The sediment load (*Sed*) is calculated by an empirical model in the literature (S. Yin et al., 2023),

$$Sed = Para_{SS} \times AS + Const_{SS} \tag{S53}$$

$$Coef_{SY} = \frac{Sed}{Pre} \tag{S54}$$

where actual streamflow (*AS*) is from *Water Supply* sector; $Para_{SS}$ and $Const_{SS}$ are derived from linear fitting of historical hydrological station data (YRCCMWR, 2020) on natural streamflow and sediment load; $Coef_{SY}$ is the coefficient of sediment yield, *Pre* is from *Climate* sector.

S2.8. Land

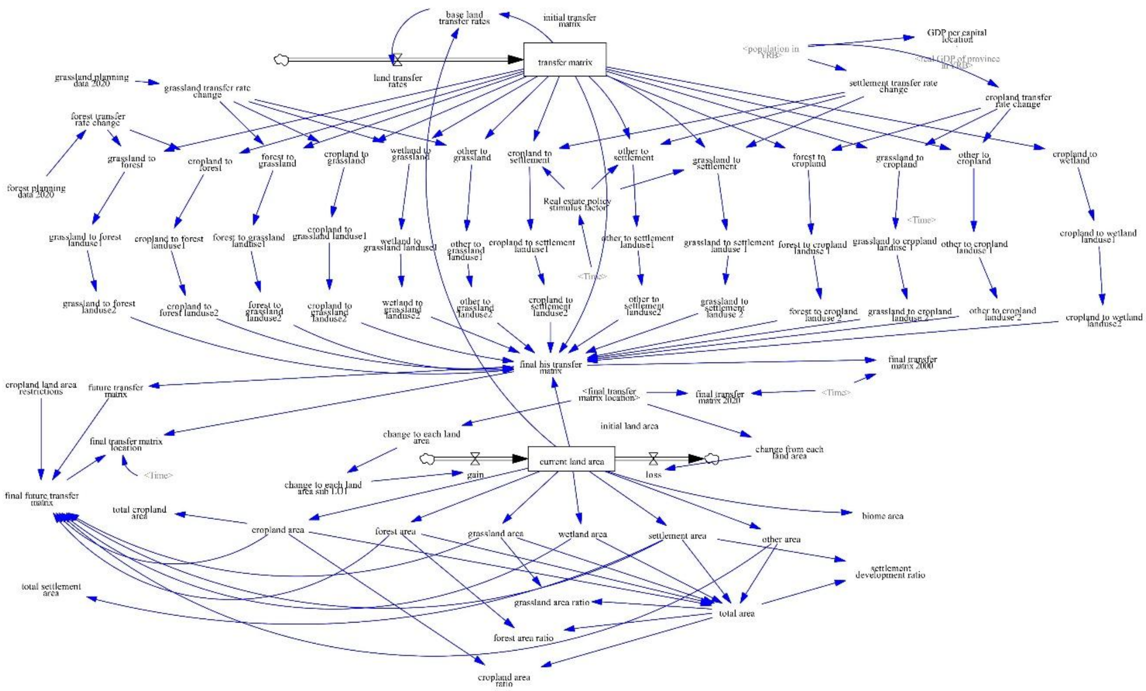

Figure S8 Model interface of *Land* sector

The *Land* sector simulates the area changes of six land use types (cropland, forest, grassland, wetland, settlement, and others), based on the transfer matrix, policies and population effects,

$$TM_{i,j} = IniTM_{i,j} + \int TMBR\, dt \tag{S55}$$

where $TM_{i,j}$ is the land use transfer matrix, indicating the area of land use *i* transfer to land use *j*, *i* and *j* represent six land use type; $IniTM_{i,j}$ is the land use transfer matrix in the initial year, *TMBR* is the base transfer rate, indicating the average annual (1981-2020) transfer area from type *i* land to type *j* land, from historical remote sensing land monitoring data (Xu et al., 2018);

The land use transfer matrix is affected by policies and population, forming the final version after calibration which is used for calculation (Equation S56),

$$FTM_{i,j} = TM_{i,j} \times Pol_{eff_i} \times Pop_{eff_i} \tag{S56}$$

$$Pol_{eff_i} = Para_{PolA_i} \times PlanArea_i \tag{S57}$$

$$Pop_{eff_i} = Para_{PopA_i} \times Pop \tag{S58}$$

where $FTM_{i,j}$ is the finial land transfer matrix, Pol_{eff} and Pop_{eff} are effects of policies and population on land transfer; $Para_{PolAi}$ is a parameter obtained by combining historical land and planning data, and $PlanArea_i$ is the historical land planning area; $Para_{PopAi}$ is the parameter derived by calibrating the model using historical land use and population data, and *Pop* is from *Population* sector;

The area of each land use type is determined by the net area after land transfers,

$$Gain_j = \sum_{i=1}^{6} FTM_{i,j} \tag{S59}$$

$$Loss_i = \sum_{j=1}^{6} FTM_{i,j} \tag{S60}$$

$$Area_i = IniArea_i + \int \left(Gain_j - Loss_i\right)dt \tag{S61}$$

where $Gain_i$ is the added area of land use *i* (i.e., the transferred in area), $Loss_i$ is the reduction of land use *i* (i.e., the transferred-out area), $IniArea_i$ is area of land use *i* in the initial year, and $Area_i$ is area of land use *i*.

S2.9. Carbon

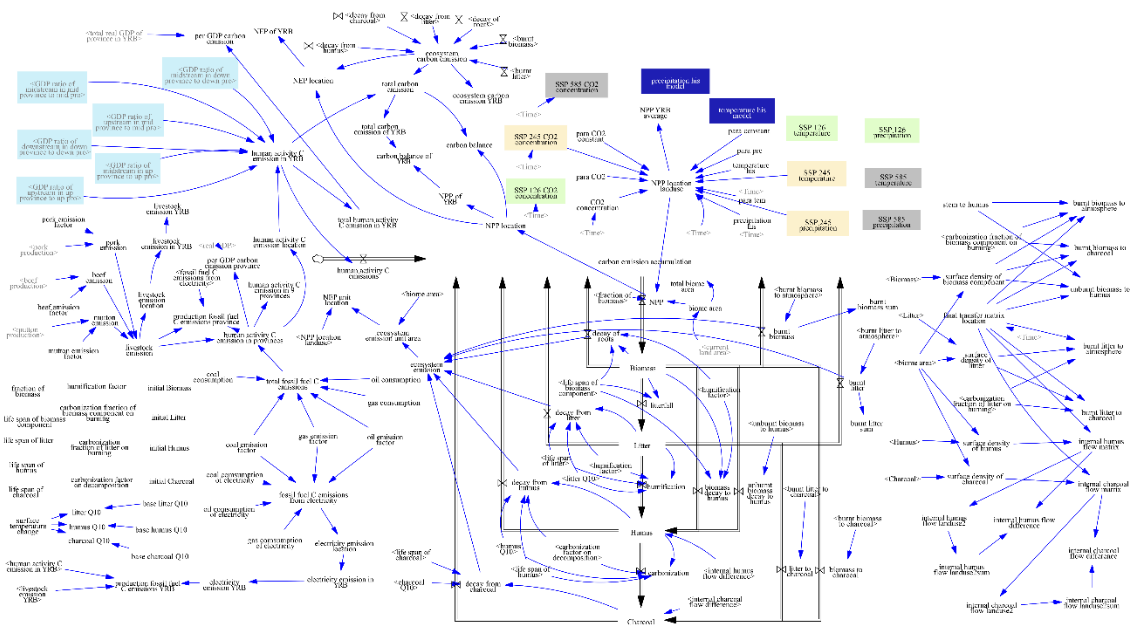

Figure S9 Model interface of *Carbon* sector

The Carbon sector simulates the basin's carbon balance processes, including carbon emission (*CE*) and absorption (*CA*). Carbon emissions (*CE*) encompass livestock emission (*LC*), and fossil fuel emissions (*FFC*), and ecosystem respiration (*BC*, *DB*, *DL*, *DH*, *DC*).

The carbon absorption (*CA*) is:

$$CA = \sum_{i=1}^{6} NPP_i \times Area_i \tag{S62}$$

where NPP_i is the net primary productivity of land use *i*, land sue area ($Area_i$) is from *Land* sector.

The net primary productivity (NPP_i) is calculated as:

$$NPP_i = Para_{co2} \times CO_2 + Const_{co2} + Para_{NT} \times Tem \times Para_{NP} \times Pre + Const_{NTP} \quad \text{(S63)}$$

where $Para_{co2}$ and $Const_{co2}$ are parameters obtained by linearly fitting historical CO_2 data with the trend component of historical NPP values from Global Vegetation Productivity Products (GVPP) (Cui et al., 2016; Wang et al., 2020; Yu et al., 2018). $Para_{NT}$, $Para_{NP}$ and $Const_{NTP}$ are derived by linearly fitting historical temperature and precipitation data with the anomaly component of historical NPP values, CO_2, *Tem* and *Pre* are CO_2 concentration, temperature and precipitation at sub-basin scale, all from *Climate* sector.

The carbon absorption (*CE*) is:

$$CE = LC + FFC + BC + DB + DL + DH + DC \quad \text{(S64)}$$

where *BC* is burning carbon emission, *DB*, *DL*, *DH* and *DC* are carbon emissions from the decay of biomass, litter, humus, and charcoal.

The livestock carbon emission (*LC*) is:

$$LC = \sum_{m=1}^{3} Livestock_{pro} \times PMR_m \times EFL_m \quad \text{(S65)}$$

where *m* represents the livestock meat type, pork, beef, and mutton, PMR_m is the share of production by livestock meat type, EFL_m is the carbon emission coefficient of livestock meat m, from the literature (Gu et al., 2023).

The fossil fuels emission (*FFC*) is:

$$FFC = \sum_{f=1}^{3} FFC_f \times EFF_f \quad \text{(S66)}$$

where *f* represents fossil fuel types, including coal, oil, gas; FFC_f is the fossil fuel consumption, from *Energy* sector, EFF_f is the carbon emission coefficient of fossil fuel *f*, from the literature (Liu et al., 2015).

The burning carbon emission (*BC*) is:

$$BC = \sum_{i=1}^{6} \left(\sum_{b=1}^{4} BCB_{i,b} + BCL_i \right) \quad \text{(S67)}$$

$$BCB_{i,b} = (1 - BCF_b) \times \frac{Bio_{i,b}}{Area_i} \times Loss_i \quad \text{(S68)}$$

$$BCL_i = (1 - LCF) \times \frac{Lit_i}{Area_i} \times Loss_i \quad \text{(S69)}$$

where *i* represent land use type; *b* represents biomass components (leaf, branch, stem, root); $BCB_{i,b}$ is the carbon emission from biomass combustion, BCL_i is the carbon emission from litter combustion; BCF_b and *LCF* are carbonization ratios, from the ANIME_Yangze model (Jiang et al., 2022); $Bio_{i,b}$ and Lit_i are biomass and litter carbon pools; the loss of land use i ($Loss_i$) and area of land use i ($Area_i$) are from *Land* sector.

The biomass carbon pools ($Bio_{i,b}$) is:

$$Bio_{i,b} = IniBio_{i,b} + \int \left(BioFra_{i,b} \times NPP_i \times Area_i - DB_{i,b} - BCB_{i,b} - DBL_{i,b} - DBH_{i,b} - UBBH_{i,b} - BBC_{i,b}\right)dt \quad \text{(S70)}$$

where $IniBio_{i,b}$ is the carbon pool storage of biomass in the initial year; $BioFra_b$ is the ratio of biomass components, from the ANIME_Yangze model (Jiang et al., 2022); NPP_i is the net primary productivity of land use i; $Area_i$ is land use i area; $DB_{i,b}$ is the carbon emission from the decay of biomass; $BCB_{i,b}$ is the carbon emission from biomass combustion, $DBL_{i,b}$ represents the amount of biomass decayed as litter, including leaves, branches, and stems, $DBH_{i,b}$ represents the amount of biomass decayed as humus, specifically for roots, $UBBH_{i,b}$ is the amount of unburned biomass (dead biomass) converted into humus, $BBC_{i,b}$ the amount of biomass converted into charcoal during combustion.

The amount of biomass decayed as litter ($DBL_{i,b}$) is:

$$DBL_{i,b} = \frac{Bio_{i,b}}{LSB_{i,b}} \quad \text{(S71)}$$

where $LSB_{i,b}$ refers to the lifespan of the biomass, obtained from the ANIME_Yangze model (Jiang et al., 2022).

The amount of biomass decayed as humus ($DBH_{i,b}$) is:

$$DBH_{i,b} = HF_i \times \frac{Bio_{i,b}}{LSB_{i,b}} \quad \text{(S72)}$$

where HF_i is humification factor upon decomposition, namely the proportions of organic matter converted into humus during decomposition, obtained from the ANIME_Yangze model (Jiang et al., 2022);

The amount of unburned biomass (dead biomass) converted into humus ($UBBH_{i,b}$) is:

$$UBBH_{i,b} = BSH_{i,b} \times \frac{Bio_{i,b}}{Area_i} \times Loss_i \quad \text{(S73)}$$

where $BSH_{i,b}$ refers to the coefficient representing the transformation of decomposed trunks into humus, from the ANIME_Yangze model (Jiang et al., 2022), the loss of land use *i* ($Loss_i$) is from *Land* sector.

The amount of biomass converted into charcoal during combustion ($BBC_{i,b}$) is:

$$BBC_{i,b} = BCF_b \times \frac{Bio_{i,b}}{Area_i} \times Loss_i \quad \text{(S74)}$$

where BCF_b is carbonization ratios, from the ANIME_Yangze model (Jiang et al., 2022), the loss of land use i ($Loss_i$) is from *Land* sector.

The litter carbon pools (Lit_i) is:

$$Lit_i = IniLit_i + \int \left(\sum_{b=1}^{4} DBL_{i,b} - DL_i - BCL_i - DLH_i - BLC_i\right) dt \quad \text{(S75)}$$

where $IniLit_i$ is the carbon pool storage of litter in the initial year; $DBL_{i,b}$ represents the amount of biomass decayed as litter (Equation S71); DL_i is the carbon emission from the decay of litter; BCL_i is the carbon emission from litter combustion (Equation S69); DLH_i is the amount of litter converted into humus, BLC_i the amount of litter converted into charcoal during combustion.

The carbon emissions from the decay of litter (DL) is:

$$DL = \sum_{i=1}^{6} DL_i = \sum_{i=1}^{6} R_L \times (1 - HF_i) \times \frac{Lit_i}{LSL_i} \quad \text{(S76)}$$

where R_L is the respiration coefficients for litter, HF_i is humification factor upon decomposition, namely the proportions of organic matter converted into humus during decomposition, $LSL_{i,b}$ refers to the lifespan of the litter, obtained from the ANIME_Yangze model (Jiang et al., 2022).

The respiration coefficients for litter (R_L) is:

$$R_d = BaseR_d^{\left(\frac{TemS - BaseTem}{10}\right)} \quad \text{(S77)}$$

where R_d is the coefficient representing respiration; R_L, R_H and R_C correspond to the respiration coefficients for litter, humus, and biochar; $BaseR_d$ is the base respiration coefficient, *BaseTem* is the temperature in the initial year, temperature at the sub-basin scale (*Tem*) is from *Climate* sector.

The amount of litter converted into humus (DLH_i) is:

$$DLH_i = R_L \times HF_i \times \frac{Lit_i}{LSL_i} \quad \text{(S78)}$$

where R_L is the respiration coefficients for litter (Equation S77); HF_i is humification factor upon decomposition, namely the proportions of organic matter converted into humus during decomposition, LSL_i refers to the lifespan of the litter, obtained from the ANIME_Yangze model (Jiang et al., 2022);

The amount of litter converted into charcoal during combustion (BLC_i) is:

$$BLC_i = LCF \times \frac{Lit_i}{Area_i} \times Loss_i \quad \text{(S79)}$$

where *LCF* is the carbonization ratio, from the ANIME_Yangze model (Jiang et al., 2022), $Area_i$ is the area of land use *i* from *Land* sector.

The carbon emissions from the decay of biomass (*DB*) are calculated as:

$$DB = \sum_{i=1}^{6} \sum_{b=1}^{4} DB_{i,b} = \sum_{i=1}^{6} \sum_{b=1}^{4} (1 - HF_i) \times \frac{Bio_{i,b}}{LSB_{i,b}} \quad \text{(S80)}$$

where HF_i is humification factor upon decomposition, namely the proportions of organic matter converted into humus during decomposition; $Bio_{i,b}$ is the biomass carbon pools (Equation S70), $LSB_{i,b}$ refers to the lifespan of the biomass, obtained from the ANIME_Yangze model (Jiang et al., 2022).

The carbon emissions from the decay of humus (*DH*) are calculated as:

$$DH = \sum_{i=1}^{6} DH_i = \sum_{i=1}^{6} R_H \times (1 - CF_i) \times \frac{Hum_i}{LSH_i} \quad \text{(S81)}$$

where R_H is the respiration coefficients for humus (Equation S77), $LSH_{i,b}$ refers to the lifespan of the humus, obtained from the ANIME_Yangze model (Jiang et al., 2022),

$$Hum_i = IniHum_i + \int (\sum_{b=1}^{4} (DBH_{i,b} + UBBH_{i,b}) + DLH_i + IFH_i - DH_i - DHC_i) dt \quad \text{(S82)}$$

where $IniHum_i$ is the carbon pool storage of humus in the initial year; $DBH_{i,b}$ represents the amount of biomass decayed as humus, specifically for roots (Equation S72); $UBBH_{i,b}$ is the amount of unburned biomass (dead biomass) converted into humus (Equation S73); DLH_i is the amount of litter converted into humus (Equation S78); IFH_i is the dynamic changes of humus in the soil; DH_i is the carbon emissions from the decay of humus (Equation S81); DHC_i is the amount of humus converted into charcoal.

The dynamic changes of humus in the soil (IFH_i) is:

$$IFH_i = \sum_{i=0}^{6} \frac{Hum_i}{Area_i} \times FTM_{i,j} - \sum_{j=0}^{6} \frac{Hum_i}{Area_i} \times FTM_{i,j} \quad \text{(S83)}$$

where final transfer matrix ($FTM_{i,j}$) and area of land use i are from *Land* sector.

The amount of humus converted into charcoal (DHC_i) is:

$$DHC_i = R_H \times CF_i \times \frac{Hum_i}{LSH_i} \quad \text{(S84)}$$

where R_H is the respiration coefficients for humus; LSH_i refers to the lifespan of the humus, obtained from the ANIME_Yangze model (Jiang et al., 2022).

The carbon emissions from the decay of charcoal (*DC*) is:

$$DC = \sum_{i=1}^{6} DC_i = \sum_{i=1}^{6} \left(R_C \times \frac{Cha_i}{LSC_i} \right) \quad \text{(S85)}$$

where Cha_i is the charcoal carbon pools. R_C is the respiration coefficients for biochar, LSC_i refers to the lifespan of the charcoal carbon pools, obtained from the ANIME_Yangze model (Jiang et al., 2022).

The charcoal carbon pools (Cha_i) is:

$$Cha_i = IniCha_i + \int \left(\sum_{b=1}^{4} DBC_{i,b} + DHC_i + DLC_i + BLC_i + IFC_i - DC_i \right) dt \quad \text{(S86)}$$

where $IniCha_i$ is the carbon pool storage of charcoal in the initial year; $DBC_{i,b}$ is amount of burnt biomass to charcoal; DHC_i is the amount of humus converted into charcoal (Equation S84); DLC_i is amount of burnt litter to charcoal; BLC_i is the amount of litter converted into charcoal during combustion (Equation S79); IFC_i represents the dynamic changes of charcoal in the soil.

The amount of biomass decayed as charcoal ($DBC_{i,b}$) is:

$$DBC_{i,b} = BCF_b \times \frac{Bio_{i,b}}{Area_i} \times Loss_i \quad \text{(S87)}$$

where BCF_b is carbonization ratios, obtained from the ANIME_Yangze model (Jiang et al., 2022); $Bio_{i,b}$ is biomass carbon pools; the loss9 of land use i ($Loss_i$) and area of land use i ($Area_i$) are from *Land* sector.

The dynamic changes of charcoal in the soil (IFC_i) is:

$$IFC_i = \sum_{i=0}^{6} \frac{Cha_i}{Area_i} \times FTM_{i,j} - \sum_{j=0}^{6} \frac{Cha_i}{Area_i} \times FTM_{i,j} \quad \text{(S88)}$$

where final transfer matrix ($FTM_{i,j}$) and area of land use *i* are from *Land* sector.

S3. Exogenous variables for the CHANS-SD-YRB model

In the model, there are more than 100 exogenous variables, some of which are initial variables that drive the simulation of stocks (Table S2). These exogenous variables are derived either from historical statistical data or from fitted results based on historical data.

Table S2 Summary of exogenous variables. Initial variable (denoted as Y) only provides a value for the first year (1981), and other exogenous variables are required to provide values for the entire simulation time range.

Sector	Exogenous variables	Initial variable
Population	• initial population	Y
	• total fertility	

	• proportion of male babies • age specific fertility distribution • average years of schooling • migration rate age proportion • China GDP per capital data • urban population share • population in Yellow River Basin ratio	
Economy	• initial industry capital • average life of industry capital • initial industry production • industry capital elasticity • initial employment • elasticity of industry productivity to health • elasticity of industry productivity to education • elasticity of industry productivity to infrastructure density • initial service capital • average life of service capital • initial service production • service capital elasticity • initial employment • elasticity of service productivity to health • elasticity of service productivity to education • initial agriculture capital • elasticity of service productivity to infrastructure density • crop value added per kg • pork value added per kg • beef value added per kg • mutton value added per kg • elasticity of sector on investment • saving share of income • government expenditure without interest share • government investment share • GDP in Yellow River Basin ratio	Y Y Y Y Y Y Y
Energy	• household electricity fitting parameters • per unit GDP electricity consumption • electricity transmit out • electricity transmit in • electricity transmission loss • fire generation share • hydro power generation share • wind generation share • solar generation share • nuclear generation share • gas consumption per rural person	

	• gas consumption per urban person • gas production fitting parameters • oil production fitting parameters • coal production fitting parameters	
Food	• fertilizer use fitting parameters • yields fitting parameters • crop multiple cropping index • crop harvest ratio • percentage of energy in urban potato diets • percentage of energy in rural potato diets • percentage of energy in urban bean diets • percentage of energy in rural bean diets • percentage of energy in urban cereal diets • percentage of energy in rural cereal diets • percentage of dietary energy from animal foods in urban regions • percentage of dietary energy from animal foods in rural regions • industrial food ratio • seed and loss food ratio	
Water Demand	• irrigation water intensity • livestock water intensity • industry water intensity • service water intensity • household water use fitting parameters	
Water Supply	• slope • underlying surface fitting parameters • vegetation coverage fitting parameters • streamflow loss coefficient • water consumption coefficient • water use in Yellow River Basin ratio	
Land	• initial transfer matrix • forest planning data • grassland planning data • cropland land area restrictions	Y
Carbon	• pork emission factor • beef emission factor • mutton emission factor • coal emission factor • gas emission factor • oil emission factor • net primary productivity fitting parameters • life span of biomass • life span of litter	

	• life span of humus	
	• life span of charcoal	
	• initial biomass	Y
	• initial span of litter	Y
	• initial span of humus	Y
	• initial span of charcoal	Y
	• fraction of biomass	
	• humification factor	
	• carbonization factor	
Sediment	• sediment load fitting parameters	
Climate	• precipitation • temperature • potential evapotranspiration • precipitation intensity • CO_2 concentration	

S4. Scale conversion of human-natural processes

This study adopts high spatial resolution gridded data and performs scale conversion between administrative-level human societal processes and sub-basin-level natural ecological processes based on the proportional relationship between sub-basins and provinces. As an example, Fig. S10 illustrates the conversion of provincial GDP into the middle reaches of the Yellow River Basin.

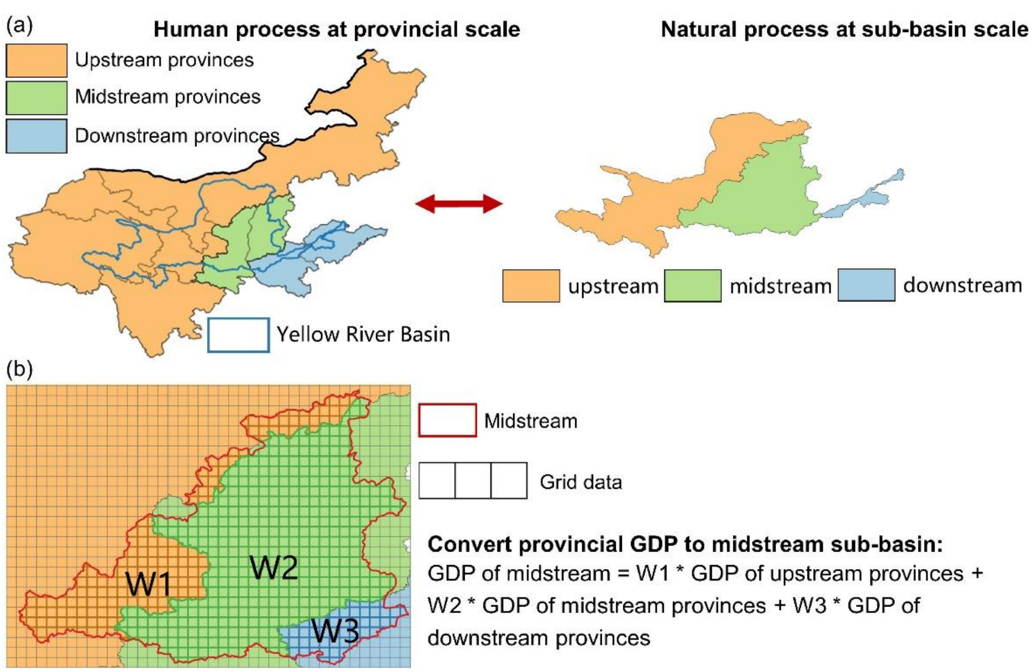

Figure S10 Spatial scale of human and natural processes in the YRB model and their conversion. (a) Human processes at provincial level and natural processes at sub-basin level. (b) Example of scale conversion between provincial and sub-basin scales for GDP. Gridded data are used to calculate weights (W1, W2, W3) of each intercepted parts of sub-basin and corresponding provinces to enable upscaling and downscaling between specific human and natural processes. Sourced from Sang et al. (2025).

Due to data limitations, not all human societal process variables are available at high spatial resolution. Therefore, scale conversion ratios for key societal variables were used as proxies for other variables since they have strong correlations (Table S3).

Table S3 Scale conversion by high spatial resolution

Variables	**Proxy gridded data**	**Spatial resolution**	**Data source**
Population	Population density grid data	1 km	Kilometer grid dataset of China's population spatial distribution (Xu, 2017b)
GDP	GDP grid data	1 km	Kilometer grid dataset of China's GDP spatial distribution (Xu, 2017a)
Carbon emission	GDP grid data	1 km	Kilometer grid dataset of China's GDP spatial distribution (Xu, 2017a)

S5. Future baseline scenario design

The future baseline scenario represents a trajectory in which existing plans and policies continue to operate without substantial changes in external environments. The development of the baseline scenario primarily relies on variables from the *Population*, *Economy*, *Water Demand*, and *Land* sector based on available government planning documents, historical trends, and other projections.

(1) Total fertility and Gender ratio

China's total fertility rate and sex ratio projected data were derived from the United Nations World Population Prospects 2024 (https://population.un.org/wpp/) which are projected using historical fertility and gender data.

(2) Average years of schooling

The upper limit of average years of schooling for each province in the Yellow River Basin (YRB) was set to the maximum observed national value in 2023 (Germany) (data from https://ourworldindata.org/grapher/mean-years-of-schooling-long-run), with annual increases estimated according to the growth rates specified in China's Five-Year Plans.

(3) Urban and rural population ratio

The urbanization rate was constrained to an upper limit of 80%, consistent with projections from the Report on the Analysis and Forecast of China’s Urbanization Trend toward Modernization (2020) (Cai and Zhang, 2021) and growth rates (1%/yr) specified in China’s Five-Year Plans.

(4) Labor force

Gradually Raising the Statutory Retirement Age Policy (https://www.gov.cn/yaowen/liebiao/202409/content_6974294.htm): Beginning in 2025, the government gradually raises the statutory retirement age over the next 15 years—from 55 to 58 for men, and from 50 to 55 for women, respectively. The model defines the working-age population in accordance with policy adjustments, which in turn influence future labor force dynamics.

(5) Electricity generation sources ratio

Carbon Peaking and Carbon Neutrality Goals (https://www.xinhuanet.com/politics/leaders/2020-09/22/c_1126527652.htm): China aims to peak carbon dioxide emissions before 2030 and achieve carbon neutrality by 2060. The model uses the provincial-level projections of energy consumption structure in China under this policy from Li et al (2024).

(6) Water use intensity

It was assumed that all irrigation employs water-saving technologies, with four irrigation methods (canal lining irrigation, pipeline irrigation, sprinkler irrigation, and drip irrigation) each accounting for 25% of the total irrigated area. Based on the irrigation quotas of these methods, the resulting irrigation intensity represents the lowest achievable level in the future and is set to decline annually by 1% until reaching this minimum.

For industrial, service, and livestock sectors, minimum water use intensities were determined based on values for high-income countries in 2022 from FAO/UN-Water SDG 6.4.1 dataset (UNSD, 2024), and were assumed to decrease by 1% per year until reaching the minimum.

(7) Land use area

Outline of the National Overall Planning on Land Use (2006 - 2020) (https://www.ndrc.gov.cn/fggz/fzzlgh/gjjzxgh/201705/t20170517_1196768_ext.html) stipulates minimum cropland area requirements for each province to prevent excessive farmland loss. The model defines a minimum threshold as the red line for cropland area.

Given that the SSP 2-4.5 climate pathway aligns most closely with projected climate trends in the Yellow River Basin, climate data from CMIP6 simulations under this scenario were used to drive the model and simulate future dynamics of the basin's natural ecosystems. Potential evapotranspiration (PET) was derived from existing datasets (Song et al., 2023), which generated by climate data from 14 CMIP6 General Circulation Models (GCMs) using the Penman-Monteith method. Considering both the models available for PET estimation and data accessibility, 11 CMIP6 models were selected: ACCESS-CM2, CESM2, CMCC-ESM2, GFDL-ESM4, INM-CM4-8, INM-CM5-0, IPSL-CM6A-LR, MIROC6, MRI-ESM2-0, UKESM1-0-LL, and HadGEM-GC31-LL. CMIP 6 model data comes from https://cds.climate.copernicus.eu/datasets/projections-cmip6?tab=download. For each model, temperature and precipitation data were obtained, and temperature, precipitation, and precipitation intensity were calculated annually at provincial and sub-basin scales. The ensemble mean of the 11 models was then used as input for the simulations. To ensure data consistency, CMIP6 climate projection historical data (1981–2014) replaced observed historical records, and CMIP6 climate projections in future (2015-2100) were used for 2015 onward.

References:

Cai, Y. and Zhang, C.: Analysis and prediction of urbanization trends in China's modernization, in: GREEN BOOK OF POPULATION AND LABOR:REPORT ON CHINA'S POPULATION AND LABOR No.22, Social Science Literature Press, 2021.

Cobb, C. W. and Douglas, P. H.: A theory of production, The American Economic Review, 18, 139–165, 1928.

Cui, T., Wang, Y., Sun, R., Qiao, C., Fan, W., Jiang, G., Hao, L., and Zhang, L.: Estimating Vegetation Primary Production in the Heihe River Basin of China with Multi-Source and Multi-Scale Data, PLOS ONE, 11, e0153971, https://doi.org/10.1371/journal.pone.0153971, 2016.

Gou, J., Miao, C., Samaniego, L., Xiao, M., Wu, J., and Guo, X.: CNRD v1.0: A High-Quality Natural Runoff Dataset for Hydrological and Climate Studies in China, Bulletin of the American Meteorological Society, 102, E929–E947, https://doi.org/10.1175/BAMS-D-20-0094.1, 2021.

Gu, S., Qiu, Z., Zhan, Y., Qian, K., Xiong, R., Dai, H., Yin, J., and Shen, W.: Spatial-temporal characteristics and trend prediction of carbon emissions from animal husbandry in China, Journal of Agro-Environment Science, 42, 705–714, https://doi.org/10.11654/jaes.2022-0666, 2023.

Jia, K., Liang, S., Liu, S., Li, Y., Xiao, Z., Yao, Y., Jiang, B., Zhao, X., Wang, X., Xu, S., and Cui, J.: Global Land Surface Fractional Vegetation Cover Estimation Using General Regression Neural Networks From MODIS Surface Reflectance, IEEE Transactions on Geoscience and Remote Sensing, 53, 4787–4796, https://doi.org/10.1109/TGRS.2015.2409563, 2015.

Jia, K., Yang, L., Liang, S., Xiao, Z., Zhao, X., Yao, Y., Zhang, X., Jiang, B., and Liu, D.: Long-Term Global Land Surface Satellite (GLASS) Fractional Vegetation Cover Product Derived From MODIS and AVHRR Data, IEEE Journal of Selected Topics in Applied Earth Observations and Remote Sensing, 12, 508–518, https://doi.org/10.1109/JSTARS.2018.2854293, 2019.

Jiang, H., Simonovic, S. P., and Yu, Z.: ANEMI_Yangtze v1.0: a coupled human–natural systems model for the Yangtze Economic Belt – model description, Geosci. Model Dev., 26, 2022.

Ju, L., Yu, D., Fang, H., Guo, Q., Xu, X., Li, S., and Zhao, L.: Trends and food sources composition of energy,protein and fat in Chinese residents,1992-2012, JOURNAL OF HYGIENE RESEARCH, 47, 1000-8020(2018)05-0689–07, 2018.

Liu, Z., Guan, D., Wei, W., Davis, S. J., Ciais, P., Bai, J., Peng, S., Zhang, Q., Hubacek, K., Marland, G., Andres, R. J., Crawford-Brown, D., Lin, J., Zhao, H., Hong, C., Boden, T. A., Feng, K., Peters, G. P., Xi, F., Liu, J., Li, Y., Zhao, Y., Zeng, N., and He, K.: Reduced carbon emission estimates from fossil fuel combustion and cement production in China, Nature, 524, 335–338, https://doi.org/10.1038/nature14677, 2015.

MAARA: China Agriculture Yearbook, https://data.cnki.net/yearBook?type=type&code=A, 2020.

Miao, C., Gou, J., Fu, B., Tang, Q., Duan, Q., Chen, Z., Lei, H., Chen, J., Guo, J., Borthwick, A. G. L., Ding, W., Duan, X., Li, Y., Kong, D., Guo, X., and Wu, J.: High-quality reconstruction of China's natural streamflow, Science Bulletin, 67, 547–556, https://doi.org/10.1016/j.scib.2021.09.022, 2022.

NBSC: China Energy Statistical Yearbook, https://data.cnki.net/yearBook?type=type&code=A, 2020a.

NBSC: China Population Census Yearbook, https://data.cnki.net/yearBook?type=type&code=A, 2020b.

NBSC: China Statistical Yearbooks, https://www.stats.gov.cn/english/, 2020c.

Qu, W., Shi, W., Zhang, J., and Liu, T.: T21 China 2050: A Tool for National Sustainable Development Planning, Geography and Sustainability, 1, 33–46, https://doi.org/10.1016/j.geosus.2020.03.004, 2020.

Sang, S., Li, Y., Zong, S., Yu, L., Wang, S., Liu, Y., Wu, X., Song, S., Wang, X., and Fu, B.: The modeling framework of the coupled human and natural systems in the Yellow River Basin, Geography and Sustainability, 6, 100294, https://doi.org/10.1016/j.geosus.2025.100294, 2025.

Song, Y. H., Chung, E.-S., Shahid, S., Kim, Y., and Kim, D.: Development of global monthly dataset of CMIP6 climate variables for estimating evapotranspiration, Sci Data, 10, 568, https://doi.org/10.1038/s41597-023-02475-7, 2023.

UNSD: SDG Indicator 6.4.1 – Change in water use efficiency over time., 2024.

Ventana Systems, Inc.: Vensim DSS (version 9.3), 2023.

Wang, M., Sun, R., Zhu, A., and Xiao, Z.: Evaluation and Comparison of Light Use Efficiency and Gross Primary Productivity Using Three Different Approaches, Remote Sensing, 12, 1003, https://doi.org/10.3390/rs12061003, 2020.

Xu, X.: Kilometer grid dataset of China's GDP spatial distribution, https://doi.org/10.12078/2017121102, 2017a.

Xu, X.: Kilometer grid dataset of China's population spatial distribution, https://doi.org/10.12078/2017121101, 2017b.

Xu, X., Liu, J., Zhang, S., Li, R., Yan, C., and Wu, S.: China land use remote sensing monitoring dataset, https://doi.org/10.12078/2018070201, 2018.

Yang, D., Shao, W., Yeh, P. J.-F., Yang, H., Kanae, S., and Oki, T.: Impact of vegetation coverage on regional water balance in the nonhumid regions of China, Water Resources Research, 45, https://doi.org/10.1029/2008WR006948, 2009.

YRCCMWR: Yellow River Water Resources Bulletin, 2020.

Yu, T., Sun, R., Xiao, Z., Zhang, Q., Liu, G., Cui, T., and Wang, J.: Estimation of Global Vegetation Productivity from Global LAnd Surface Satellite Data, Remote Sensing, 10, 327, https://doi.org/10.3390/rs10020327, 2018.

Zeng, X., Zhang, Z., Wang, J., and Zhao, Y.: Analysis and Prospect of China's Food Consumption, Agricultural Outlook, 17, 104–114, 2021.

Zhang, Y., Cao, Y., and Lin, W.: Estimation on Grain Consumption Gap Between Urban and Rural Areasin China, Journal of Northwest A&F University (SocialScienceEdition), 12, 1009-9107(2012)04-0050–07, https://doi.org/10.13968/j.cnki.1009-9107.2012.04.021, 2012.